Constructing the Universe with Clusters of Galaxies, IAP 2000 meeting, Paris (France) July 2000
Florence Durret & Daniel Gerbal eds.

DYNAMICS OF THE X-RAY CLUSTERS ABELL 222, ABELL 223 AND ABELL 520 [a]

D. PROUST(1), L. SODRE Jr.(2), H. CUEVAS(3), H.V. CAPELATO(4) and B. TOME LEHODEY(4)

(1) DAEC Observatoire de Paris-Meudon, 92195 Meudon Cedex, France
(2) Departamento de Astronomia IAG/USP, Av. Miguel Stefano 4200, 04301-904, São Paulo, Brazil
(3) Universidad de La Serena, Av. Benavente 980, La Serena, Chile
(4) Divisão de Astrofisica INPE/MCT, 12225-010, São José dos Campos, Brazil

We present the results of a dynamical analysis as well as the population content of three rich, X-ray luminous galaxy clusters, Abell 222, Abell 223 and Abell 520, that are at intermediate redshifts.

1 Spatial distribution and kinematical properties

As already noticed by Sandage, Kristian & Westphal 1976[12], the two neighboring clusters A222 and A223 have nearly the same redshift and probably constitute an interacting system which is going to merge in the future. Both are dominated by a particularly bright cD galaxy. They have a richness class R=3 and are X-ray luminous with $L_X(7\ \mathrm{keV}) = 3.7 \pm 0.7\ 10^{44}$ erg s^{-1} and $1.5 \pm 0.6\ 10^{44}$ erg s^{-1} for A222 and A223, respectively (Lea & Henry, 1988)[8]. Isophotes of a wavelet reconstruction (Rué & Bijaoui, 1997)[11] of a ROSAT HRI X-ray image, superposed on the significance maps of the projected density of galaxies were obtained for the two clusters (Proust *et al.* 2000)[9]. These maps were constructed by taking galaxies from the deeper Butcher, Oemler & Wells 1983[3] (BOW83) catalog, which is complete up to $f_{57} \sim 22$. They show that the general structure of both clusters A222 and A223 is extremely complex, presenting several clumps of galaxies in projection on their central regions. The X-ray emission is centered, for both clusters, in their main galaxy concentrations, but this does not correspond to location of their brightest members, as it is usually observed in nearby rich clusters of galaxies. All these pieces of data support the view that we are facing a dynamically unrelaxed, young system.

We have used the ROSTAT statistical package (Beers *et al.* 1990[2]; Ribeiro *et al.* 1998[10]) to analyze the velocity distributions obtained from a sample of 50 galaxies with measured velocities. Its mean velocity is $V_{bi} = 63833 \pm 165$ km s^{-1}, with dispersion $\sigma_{bi} = 1157 \pm 119$ km s^{-1}. This places the system at redshift $z = 0.21292$. The A222 galaxies have slightly higher velocities than those of A223: mean velocities are $V_{bi} = 64242 \pm 194$ km s^{-1}, for A222, and $V_{bi} = 63197 \pm 266$ km s^{-1} for A223.

The analysis of A520 data proceeded in the same lines as that of the A222+A223 system. We also obtained the X-ray isophotes of a wavelet reconstruction of the ROSAT/HRI image of A520, superposed to the significance map of the projected density of galaxies (Proust *et al.* 2000[9]). The A520 cluster, as for A222/223, may be an example of a dynamically young system where clumps of galaxies are still in phase of collapsing on its dark matter gravitational well, probably located at the mean center of the X-ray emission region seen in Figures 2, 3 and 6 of Proust *et al.* 2000[9]. The mean velocity for this sample with 21 retained galaxies is $V_{bi} = 60127 \pm 284$ km s^{-1}, with dispersion $\sigma_{bi} = 1250 \pm 189$ km s^{-1}, placing the cluster at redshift $z = 0.20056$.

Table 1 gives mass and mass-luminosities ratio estimates for each cluster separately, obtained with the virial and projected mass estimators (see Table caption). Total j luminosities were estimated from the BOW83 catalog, which is complete up to $j = 22$.

[a] based on observations made at ESO-La Silla (Chile), at the Canada France Hawaii Telescope and at the Pic du Midi Observatory (France).

Table 1: Mass and M/L estimates

(1) Cl.	(2) R	(3) L_j	(4) N_L	(5) N_v	(6) Mass Virial	(6) Mass Proj.	(7) M/L Virial	(7) M/L Proj.	(8) N
A222	200"	1.15	107	27	7.55 ± 2.56	10.05 ± 3.39	658	876	a
					2.85	5.22 ± 1.29	248	450	b
	350"	1.46	140	30	8.08 ± 2.60	10.25 ± 3.27	553	701	a
					2.91	5.30 ± 1.24	199	363	b
A223	200"	1.13	84	10	6.69 ± 3.73	12.69 ± 7.02	686	11230	a
					3.84	7.05 ± 2.97	340	624	b
	350"	1.49	124	16	10.17 ± 4.47	19.62 ± 8.58	684	13190	a
					5.50	10.46 ± 3.41	370	731	b
A520	200"	2.57	166	16	12.33 ± 5.42	16.74 ± 7.33	481	625	a
					6.71	8.93 ± 2.91	261	348	b
	350"	3.78	234	20	15.73 ± 6.19	20.91 ± 8.18	428	569	a
					8.01	11.01 ± 3.19	218	300	b

column(1): Cluster Name, column(2): radius in arcsec., column(3): total luminosity with $j < 22$ in $10^{12} h_{50}^{-2} L_{\odot}$, column(4): number of galaxies with j < 22, column(5): number of galaxies with measured velocity, column(6): mass of the cluster in $10^{14} h_{50}^{-1} M_{\odot}$, column(7): mass-luminosity ratio in solar units, column(8): mass estimators: (a) self-gravitating system (Heisler 1985[7]), (b) test particle system (Bahcall & Tremaine 1981[1])

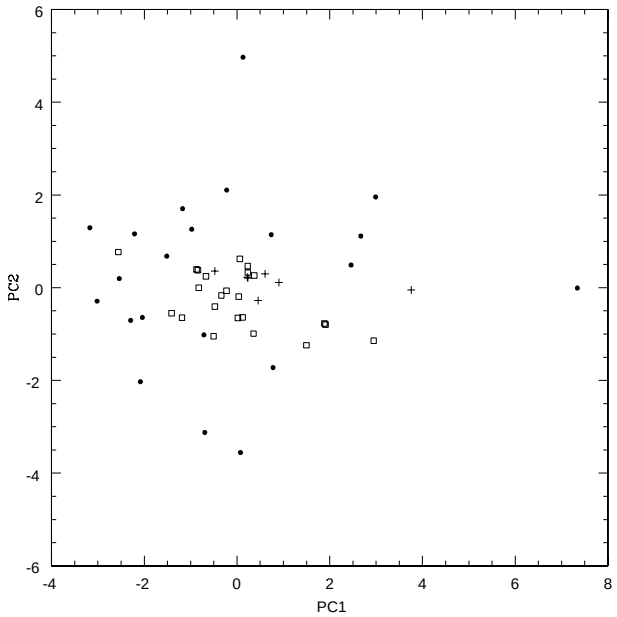

Figure 1: Projection of the spectra of A222, A223 and A520 onto the first two principal components of the galaxies. Different symbols correspond to different signal-to-noise ratios, computed in the wavelength interval between 4500Å and 5000Å. Filled circles: $2.9 \leq S/N < 5.5$; squares $5.5 \leq S/N < 8.0$; crosses: $S/N \geq 8.0$.

2 Spectral Classification

Spectral classification has been performed through a Principal Component Analysis (PCA) of the spectra (Sodré & Cuevas 1994[14], 1997[15]; Connolly *et al.* 1995[4]; Folkes *et al.* 1996[6]). The spectral sequence correlates well with the Hubble morphological sequence, and we define the "spectral type" (hereafter ST) of a galaxy from its position along the spectral sequence (defined by the first principal component). Following Sodré & Cuevas 1997[15], we apply this method to a sample of 51 CFHT spectra of galaxies that are probably members of the clusters A222, A223 and A520 (section 3) to obtain spectral types. Figure 1 shows the projection of the spectra of the 51 galaxies of the three clusters onto the plane defined by the first two principal components. In this figure, early-type galaxies are at the left side, and increasing values of ST (or, equivalently of the first principal component) correspond to later-type galaxies.

3 Morphological and Kinematical Segregation

Figure 2 (up) shows the logarithm of the projected local density normalized by a median density of each cluster versus the spectral type. This figure shows that, for A222, A223 and A520, early-type galaxies tend to be located in denser regions than late-type galaxies, indicating that the morphology-density relation (Dressler 1980)[5], as inferred using spectral types, was already established in clusters at $z \sim 0.2$. The correlation shown is significant: the Spearman rank-order correlation coefficient is r_s = -0.41 and the two-sided significance level of its deviation from zero is $p = 0.002$. Nearby clusters also present a kinematical segregation (Sodré *et al.* 1989)[13]. This may be an evidence that late-type galaxies have arrived recently in the cluster and are not yet virialized, while the early-type galaxies constitute a relaxed systems with a low velocity dispersion. Figure 2 (down) shows, as a function of spectral type, the absolute value of galaxy velocities relative to the clusters mean velocity, normalized by the velocity dispersion of each cluster. The data indicate that early-type galaxies tend to have lower relative velocities than galaxies of later types; the Spearman rank-order correlation coefficient r_s is now 0.39 and the two-sided significance level of its deviation from zero is 0.005. Hence, these clusters seem to present the same kind of kinematical segregation detected in low redshift galaxy clusters. The detailed observations and analyses can be found in Proust *et al.* 2000[9].

1. Bahcall J.N., Tremaine S., 1981, ApJ, 244,805.
2. Beers T.C., Flynn K., Gebhart K., 1990, AJ, 100, 32.
3. Butcher H., Oemler A., Wells D.C., 1983, ApJS, 52, 183 (BOW83).
4. Connolly A.J., Szalay A.S., Bershady M.A., Kinney A.L., Calzetti D., 1995, AJ, 110, 1071.
5. Dressler A., 1980, ApJS, 42, 565.
6. Folkes S.R., Lahav O., Maddox S.J., 1996, MNRAS, 283, 651.
7. Heisler J., Tremaine S., Bahcall J.N., 1985, ApJ, 298, 8.
8. Lea S.M., Henry J.P., 1988, ApJ, 332, 81.
9. Proust D., Cuevas H., Capelato H.V., Sodré Jr L., Tomé Lehodey B., Le Fèvre O., Mazure A., 2000, AA, 355, 443.
10. Ribeiro A.L.B., de Carvalho R.R., Capelato H.V., Zepf S.E., 1998, ApJ, 497, 72.
11. Rué F., Bijaoui A., 1997, Experim. Astron., 7, 129.
12. Sandage A., Kristian J., Westphal J.A., 1976, ApJ, 205, 688.
13. Sodré L., Capelato H.V., Steiner J.E., Mazure A., 1989, AJ, 97, 1279.
14. Sodré L., Cuevas H., 1994, Vistas in Astronomy, 38, 287.
15. Sodré L., Cuevas H., 1997, MNRAS, 287, 137.

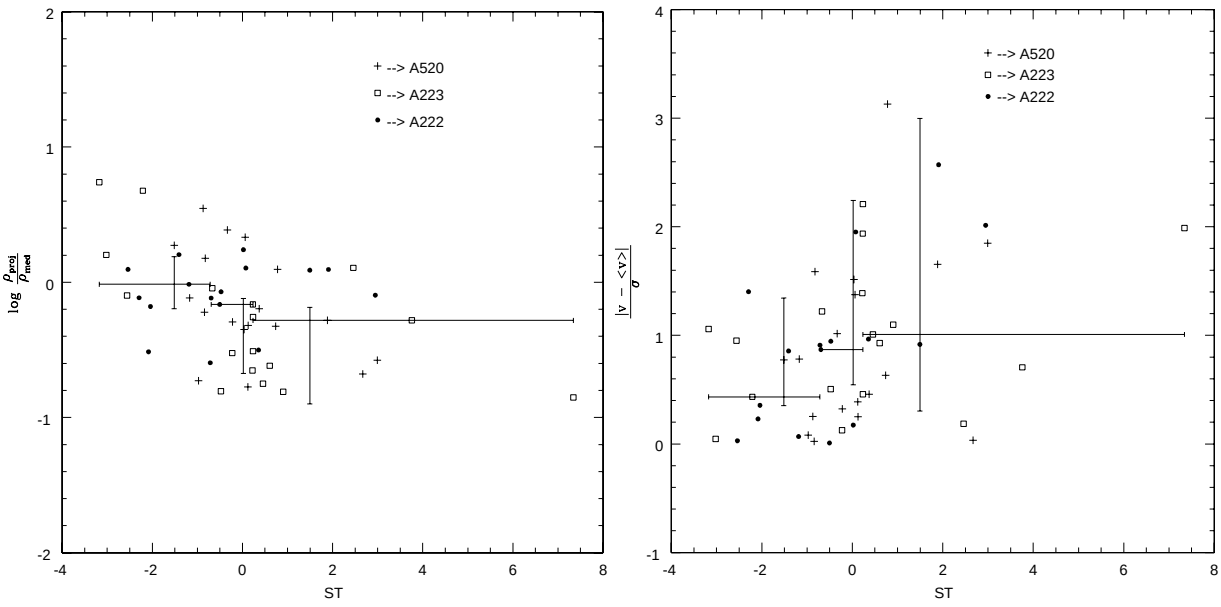

Figure 2: Up: projected local density normalized by the median density of each cluster versus the spectral type. The points with error bars are the median values taken in bins of equal galaxy number. Down: Velocity corrected to the cluster mean velocity and normalized by the velocity dispersion of each system versus the spectral type. The three clusters are plotted together, with different symbols corresponding to different clusters The vertical error bars correspond to the quartiles of the distribution, whereas the horizontal error bars indicate the interval of ST associated to each bin. Different symbols correspond to data of different clusters.